



Label-free high-throughput assays to screen and characterize novel lactate dehydrogenase inhibitors



Erica VanderPorten^a, Lauren Frick^b, Rebecca Turincio^a, Peter Thana^a, William LaMarr^b, Yichin Liu^{a,*}

^a Biochemical and Cellular Pharmacology, Genentech, South San Francisco, CA 94080, USA

^b Life Science Solutions, Agilent Technologies, Wakefield, MA 01880, USA

ARTICLE INFO

Article history:

Received 25 March 2013

Received in revised form 30 June 2013

Accepted 1 July 2013

Available online 16 July 2013

Keywords:

High-throughput screen

Lactate dehydrogenase

Mass spectrometry

Fluorescence kinetic assay

ABSTRACT

Catalytic turnover of pyruvate to lactate by lactate dehydrogenase (LDH) is critical in maintaining an intracellular nicotinamide adenine dinucleotide (NAD⁺) pool for continuous fueling of the glycolytic pathway. In this article, we describe two label-free high-throughput assays (a kinetic assay detecting the intrinsic reduced nicotinamide adenine dinucleotide (NADH) fluorescence and a mass spectrometric assay monitoring the conversion of pyruvate to lactate) that were designed to effectively identify LDH inhibitors, characterize their different mechanisms of action, and minimize potential false positives from a small molecule compound library screen. Using a fluorescence kinetic image-based reader capable of detecting NADH fluorescence in the ultra-high-throughput screening (uHTS) work flow, the enzyme activity was measured as the rate of NADH conversion to NAD⁺. Interference with NADH fluorescence by library compounds was readily identified during the primary screen. The mass spectrometric assay quantitated the lactate and pyruvate levels simultaneously. The multiple reaction monitoring mass spectrometric method accurately detected each of the two small organic acid molecules in the reaction mixture. With robust *Z'* scores of more than 0.7, these two high-throughput assays for LDH are both label free and complementary to each other in the HTS workflow by monitoring the activities of the compounds on each half of the LDH redox reaction.

© 2013 Elsevier Inc. All rights reserved.

Cancer cells have been shown to have an altered metabolism to meet the demands of faster cell division and higher energy consumption [1–3]. The altered metabolism in cancer cells is often accompanied either by a change in the expression level of an enzyme or its isoform or by an introduction of mutations or different posttranslational modification patterns that can affect functional activity of a given protein. For example, the biosynthetic pathways involved in generating fatty acids or nucleotides can be up-regulated to supply these building blocks in the fast proliferating cancer cells [4,5]. In many tumor cells, an increase in the aerobic glycolytic flux and a reduction in the oxidative phosphorylation of glucose metabolism in mitochondria was observed; these phenomena are known as the Warburg effect [6,7]. Several oncogenes such as Akt, Myc, and Ras have been linked to the Warburg effect and can activate the aerobic glycolysis pathways [8]. In addition, the loss of tumor suppressor genes such as p53 can cause a switch from cellular respiration to aerobic glycolysis, directly contributing to the Warburg effect [9,10]. The increase in the glucose uptake and glycolytic flux allows the tumor cells to quickly produce ATP as an energy source through the conversion of glucose to pyruvate,

especially under hypoxic conditions that fast-growing solid tumor cells often experience. For every glucose molecule that is consumed, glycolysis reduces two molecules of nicotinamide adenine dinucleotide (NAD⁺)¹ to reduced nicotinamide adenine dinucleotide (NADH) in order to generate two molecules of ATP. To continue fueling this glycolytic pathway in tumor cells, NADH needs to be efficiently recycled back to NAD⁺. The decrease in aerobic glucose metabolism in the mitochondria of tumor cells also reduces NADH oxidation by the TCA cycle; thus, an alternative reaction is required. Under anabolic conditions, the conversion of the NADH back to NAD⁺ is catalyzed by lactate dehydrogenase (LDH), and this oxidation is coupled to the reduction of the glycolytic product pyruvate to lactate, which will then be secreted from the cells. In many glycolytic-addicted tumor cells, the expression of LDH (especially the isoform LDHA) is found to be elevated [11,12].

¹ Abbreviations used: NAD⁺, nicotinamide adenine dinucleotide; NADH, reduced nicotinamide adenine dinucleotide; LDH, lactate dehydrogenase; LDHA, lactate dehydrogenase A; uHTS, ultra-high-throughput screening; BGG, bovine gamma globulin; TCEP, tris(2-carboxyethyl)phosphine; FDSS, Functional Drug Screening System; Hepes, 4-(2-hydroxyethyl)-1-piperazineethanesulfonic acid; DTT, dithiothreitol; RFU, relative fluorescence unit; DMSO, dimethyl sulfoxide; MRM, multiple reaction monitoring; SPE, solid-phase extraction; AUC, area under the curve.

* Corresponding author. Fax: +1 650 467 8091.

E-mail address: liu.yichin@gen.com (Y. Liu).

The enzymatic reaction catalyzed by LDH has been characterized since the 1960s, with numerous publications primarily using the detection of NADH absorbance or intrinsic fluorescence. The enzyme family is capable of carrying out both the forward (pyruvate to lactate) and reverse (lactate to pyruvate) reactions, with the preference varying among different LDH isoforms [13,14]. Furthermore, the forward enzymatic reaction has been shown to proceed as an ordered reaction, with the enzyme binding NADH first followed by the substrate, pyruvate [13,14]. Because of the ability to use NADH or NAD⁺ as substrate, LDH was used extensively as coupling enzymes for NADH or NAD⁺ detection. Even though the elevated expression of LDH in cancer had been noted a few decades ago [15], it was not until 2006 when Fantin and coworkers demonstrated the link between LDHA and tumor metabolism [16] that the LDH enzyme was transformed from a supporting role of being used in coupling enzyme assays to center stage and being used as a potential therapeutic target for cancer. This also explains in part why there has been a lack of validated inhibitors for LDH despite the fact that this enzyme has been well characterized for decades. Until recent months, the only validated inhibitor known to LDH is a small organic acid, oxamate, which is a pyruvate mimetic with a reported biochemical IC₅₀ ranging from 17 to 150 μM, depending on the assay conditions [17,18]. This weak and nonselective inhibitor that has poor cell permeability is less than an ideal tool compound for target validation in cells or *in vivo*.

With an increasing interest in exploring metabolic pathways for potential cancer therapeutic strategies, we sought to develop assay platforms that are amenable to ultra-high-throughput screening (uHTS) to identify chemical tool compounds with various mechanisms to probe the effect of LDH inhibition on cancer cell growth. LDHA has been implicated in disease progression for tumor cells that rely on glycolytic flux to provide the requisite fast energy source. LDHA is expressed to efficiently recycle NADH back to NAD⁺ to continue fueling glycolysis; thus, the enzyme has been found to drive the reaction in the forward direction (i.e., pyruvate to lactate and NADH to NAD⁺) [16,19]. Using LDHA that carries out predominantly the forward reaction as a model target, here we describe a robust 1536-well NADH fluorescence kinetic assay for screening and characterizing LDHA inhibitors. To avoid the potential for fluorescence interference from the use of NADH fluorescence as a readout, we optimized the protocol to readily identify compound fluorescence interference observed at the excitation and emission wavelengths of NADH. We also describe a label-free mass spectrometric assay set up to monitor the conversion of pyruvate to lactate by LDHA. This label-free assay was complementary to the higher throughput NADH fluorescence assay because it detected pyruvate to lactate conversion and was effective in further eliminating fluorescence artifacts as well as in identifying additional false positive mechanisms of inhibition. Finally, taking advantage of the well-characterized ordered enzyme reaction, the primary screening assay was designed to capture, and has successfully identified, uncompetitive or non-competitive inhibitors with the NADH–LDHA complex in addition to conventional inhibitors that are competitive with the substrates.

Materials and methods

Chemicals

NADH was purchased from Roche Diagnostics (Indianapolis, IN, USA). Oxamate, pyruvate, bovine gamma globulin (BGG), tris(2-carboxyethyl)phosphine (TCEP), NaCl, and Triton X-100 were obtained from Sigma–Aldrich (St. Louis, MO, USA).

1536-Well kinetic LDHA FDSS assay for primary HTS and IC₅₀ confirmation

The HTS screen was conducted on a BioCel 900 automated system outfitted with a Direct Drive Robot (Agilent Automation Solutions, Santa Clara, CA, USA). An FDSS (Functional Drug Screening System) 7000 kinetic fluorescence reader with onboard dispenser (Hamamatsu, Bridgewater, NJ, USA) was integrated with this system, enabling a fully automated workflow, including reagent additions, incubations, and detection.

Prior to the start of the screening campaign, assay-ready plates were prepared using a dedicated plate replication automation system. Using an Echo 555 acoustic dispenser (Labcyte, Sunnyvale, CA, USA), 50 nl per well of 1 mM compound was spotted onto 1536-well low-base, clear-bottom black microplates (Brooks Life Science Systems, Poway, CA, USA) and sealed using an Agilent PlateLoc microplate sealer to prevent evaporation. The sealed plates were then loaded onto the BioCel for processing. The plate seal was removed using an XPeel automated microplate seal removal device (Brooks Life Science Systems), followed by the addition of 6 μl of suspension buffer containing 50 mM Hepes buffer (pH 7.2), 0.01% Triton X-100, and 2 mM dithiothreitol (DTT) using a MultiDrop Combi dispenser (Thermo Scientific, Waltham, MA, USA). Next, 2 μl of 250 μM NADH with 10 nM C-terminally His-tagged full-length LDHA enzyme in reaction buffer A (50 mM Hepes [pH 7.2], 0.01% Triton X-100, and 0.1% BGG) was added using a BioRAPTR dispenser (Beckman Coulter, Indianapolis, IN, USA). The full-length LDHA (A2-F332) was purified as a tetramer from an *Escherichia coli* expression system using nickel–nitrilotriacetic acid (Ni–NTA) and size exclusion chromatography and stored as aliquots in storage buffer (10 mM Tris [pH 8.5], 150 mM NaCl, 45% glycerol, and 0.25 mM TCEP) at –80 °C. For control inhibition, 250 μM oxamate was included in the NADH and LDHA mixture. The plate was then centrifuged using a VSpin Microplate Centrifuge (Agilent Automation Solutions). Following a 10-min incubation at room temperature, the plate was loaded into the FDSS 7000 reader for an initial baseline read of 5 s. The onboard 1536-well pipette head of the FDSS 7000 was then used to transfer 2 μl of 250 μM pyruvate in reaction buffer A from an AutoFill refill reservoir (Acorn Instruments, South San Francisco, CA, USA) to the assay plates. The final concentration of test compound in the screen was 5 μM. Fluorescence was measured at an excitation wavelength of 340 nm and an emission wavelength of 482 nm, with one read taking place each second for a total of 3 min.

The kinetic traces were analyzed by in a Genedata Screener Kinetic Analyzer (Basel, Switzerland) using the robust slope curve fit. The slopes of the kinetic traces were calculated using a time-frame of 60 to 120 s of the aggregated data. The baseline NADH fluorescence intensity was typically measured at 300 to 400 relative fluorescence units (RFU). Fluorescent compounds with RFU values greater than 500, which was the upper limit of the linear detection range in the FDSS 7000, were excluded. The remaining compounds with more than 50% inhibition were selected for IC₅₀ confirmation. A hit rate of less than 0.1% was achieved after removing fluorescent artifacts. Average plate Z' scores were 0.7 (% LDHA activity with enzyme = 99.6 ± 5.8 and without enzyme = 0.3 ± 3.8), with reproducible NADH fluorescence window and oxamate inhibition from run to run.

384-Well IC₅₀ confirmation assay using a combination of FDSS 7000 and mass spectrometric methods

IC₅₀ follow-up by the mass spectrometric assay was conducted with compounds serially diluted in an 8-point dose response in 384-well clear-bottom black microplates. In a final reaction volume of 50 μl, 0.25 nM LDHA was incubated with 75 μM pyruvate

and 50 μM NADH in reaction buffer B (20 mM Tris [pH 7.5], 0.005% Triton, 0.005% BGG, and 2 mM DTT) and NADH fluorescence was first measured for approximately 9 min in the FDSS 7000 to reach approximately 30% conversion of pyruvate to lactate. To characterize a compound's mode of inhibition, additional experiments were conducted to determine whether compounds were pyruvate competitive or NADH competitive. To identify pyruvate-competitive inhibitors, 0.25 nM LDHA was reacted with 75 μM NADH and 500 μM pyruvate, and the IC_{50} was compared with a reaction with 75 μM NADH and 75 μM pyruvate. Reactions were read in the NADH fluorescence kinetic assay for 4.5 min and also resulted in 30% conversion of NADH to NAD^+ . Similarly, to identify NADH-competitive inhibitors, 0.25 nM LDHA was reacted with 300 μM NADH and 75 μM pyruvate and read for 4.5 min to achieve 30% conversion of pyruvate to lactate. The 50- μl reactions from the NADH fluorescence kinetic assay were quenched with 5 μl of 10% formic acid at the end of the kinetic measurement. A 50- μl aliquot of the final reaction mixture was transferred to a 384-well Greiner polypropylene clear V-bottom plate and stored at -20°C until ready to be shipped in dry ice packages to Agilent Technologies (Wakefield, MA, USA). The enzymatic activity measured by NADH fluorescence was analyzed using a Genedata Kinetic Analyzer as described above. Data were analyzed by normalizing to no-enzyme control and dimethyl sulfoxide (DMSO) control and were represented as percentage inhibition.

SPE and mass spectrometric detection

Lactate and pyruvate levels in the LDHA samples were analyzed on a RapidFire 300 High-Throughput Mass Spectrometry System (Agilent) coupled to an AB Sciex API 4000 triple-quadrupole mass spectrometer (AB Sciex, Foster City, CA, USA). The API 4000 was fitted with an electrospray ionization source and was run in negative multiple reaction monitoring (MRM) mode for the detection of lactate and pyruvate. The instrument aspirated aliquots of each sample from microplates sequentially, removing sample until the sip sensor determined that the 10- μl loop was full (usually ~ 200 ms). The contents of the loop were then applied to a solid-phase extraction (SPE) cartridge packed with a hydrophilic interaction chromatography (HILIC) material and washed with 90% acetonitrile supplemented with 10 mM ammonium acetate for 2.5 s. The purified sample was then reverse-eluted in 40% acetonitrile supplemented with 10 mM ammonium acetate in a 5-s elution step, and the eluent was sent to the mass spectrometer, which was already monitoring the mass transitions of interest. A reequilibration of 2 s brought the total cycle time to approximately 12 s. Data analysis was performed using RapidFire Integrator version 3.4 software (Agilent), which generated an output file of integrated peak areas (areas under the curve, AUCs) for each MRM transition for each sample. Percentage conversion was calculated as follows: $100 * [\text{Product AUC}/(\text{Product AUC} + \text{Substrate AUC})]$.

Results and discussion

Complementary assay strategies for detecting LDHA enzymatic activity

LDHA catalyzes the glycolytic interconversion of pyruvate and lactate, a transformation that is coupled to the redox reaction between NADH and NAD^+ (Fig. 1). Because NADH is intrinsically fluorescent, with a characteristic excitation maximum at 340 nm and an emission maximum at 480 nm (Fig. 1), it has been historically used to monitor LDH activity. Despite NADH fluorescence being a common detection method in characterizing NADH-dependent enzyme reactions, it is generally an undesirable method in screening small molecule inhibitors due to the high incidence of fluorescence

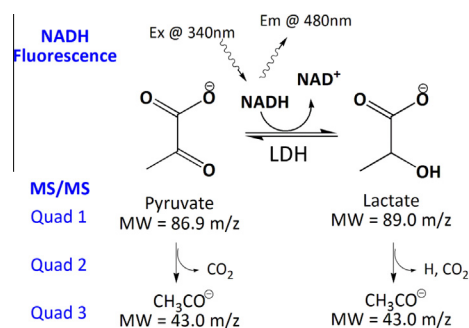


Fig. 1. An overview of the LDHA enzyme reaction and the two assays detecting the substrates and products. NADH was measured by its fluorescence (excitation at 340 nm and emission at 480 nm), whereas lactate and pyruvate were detected using mass spectrometry with their respective MRM shown.

interference at the wavelengths of NADH detection, which poses challenges in identifying true inhibitors among false positives and negatives. A well-designed kinetic measurement, however, can provide crucial information to determine how compound fluorescence might have masked the true enzyme activity via either the consumption or generation of NADH. Complementary to the NADH fluorescence detection is the measurement of pyruvate conversion to lactate (Fig. 1). Similar to NADH quantitation, a few enzyme-coupled detection methods for either pyruvate or lactate have been published [20]. Although some of the approaches can be fairly sensitive, the inhibition of the coupling enzyme in a small molecule library screen can significantly complicate the hit triage and confirmation against the target enzyme. Instead, we have taken the mass spectrometry approach to measure pyruvate and lactate. Using MRM on a triple-quadrupole mass spectrometer, pyruvate and lactate were detected by isolating parent negative ions of 86.9 and 89.0 m/z , respectively, in quad 1 followed by fragmentation in quad 2 and detection of the 43.0 m/z daughter ions in the third quad (Fig. 1).

Quantitative detection of pyruvate and lactate in mass spectrometry

The mass spectrometric assay that was developed to measure LDHA activity and inhibition detected the conversion of pyruvate to lactate. Pyruvate and lactate are both small organic acids that differ from each other by only 2.1 Da. MRM methods were established for each analyte for quantitative analysis as described above (Fig. 1). The mass spectrometer (TripleQuad AB Sciex 4000) was coupled to an Agilent RapidFire 300 system, which is an SPE platform capable of processing samples every 10 to 12 s. The analytes were first cleaned on the RapidFire system under normal-phase chromatographic conditions prior to mass spectrometric detection. The titration of each acid showed concentration-dependent intensity of the daughter ions from the targeted fragmentation of their respective parent ions as well as good detection linearity (Fig. 2A and B). The limit of quantitation for both lactate and pyruvate was 1 μM . The replicates of each titration also demonstrated solid reproducibility of the mass signals. Furthermore, the daughter ion mass signal from lactate was shown to be negligible during a titration of pyruvate (Fig. 2C), suggesting that in spite of the small mass difference between lactate and pyruvate, the detection of the mass for each acid was specific. There was also a lack of background signal in the pyruvate detection channel when a lactate titration was performed (Fig. 2D), further validating our mass spectrometry detection method. A time course of the enzymatic reaction carried out at 50 μM NADH and 75 μM pyruvate demonstrated good linearity of the reaction progress curve (Fig. 2E). Using the mass spectrometric assay allowed us to measure the potency of compounds

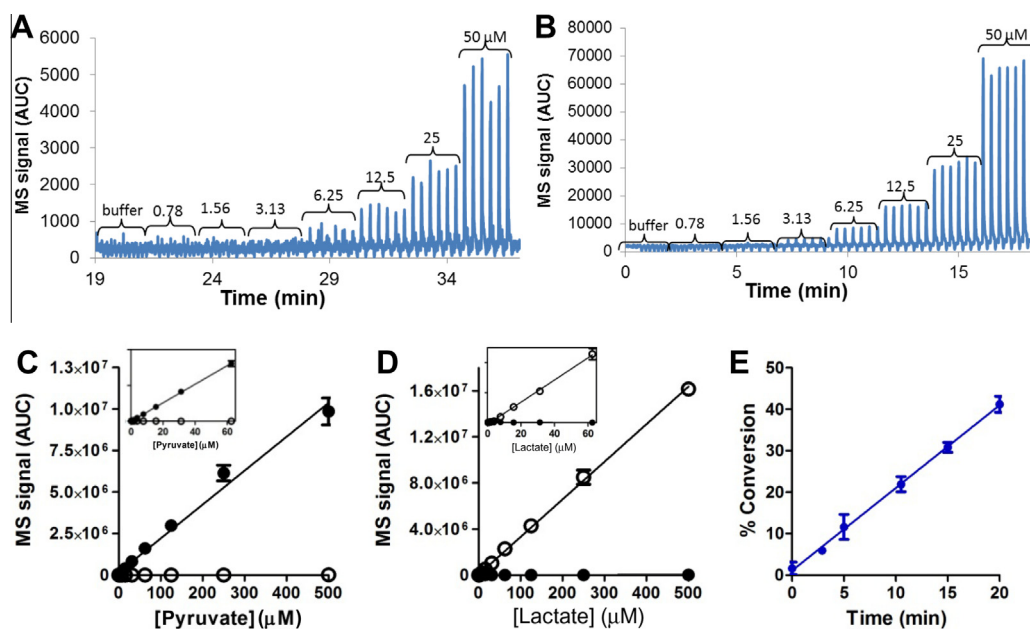


Fig. 2. (A,B) Titration of pyruvate (A) and lactate (B) in replicates in mass spectrometric assay. (C,D) Mass spectrometric signal of pyruvate MRM (C) and lactate MRM (D). The titrations of pyruvate (closed circles) and lactate (open circles) were linear, and the MRM detection was specific to each acid. The linearity is shown in the insets for lower concentrations of the analytes. (E) The LDHA reaction (0.25 nM LDHA with 75 μM pyruvate and 50 μM NADH) showed good reaction kinetic linearity up to 20 min in mass spectrometric assay. Approximately 30% conversion was achieved after 10 min of reaction, consistent with the conversion observed in NADH fluorescence kinetic assay.

that had mild fluorescence interference with NADH, to confirm true hits, and to characterize mechanism of action.

NADH fluorescence kinetic assay

The LDHA fluorescence kinetic assay was set up in a 1536-well format for the primary library screen. Because LDHA preferentially converts pyruvate and NADH to lactate and NAD^+ with very minimal activity observed in the reverse direction (data not shown), the NADH fluorescence assay is a signal loss assay. The change in NADH fluorescence was monitored using a Hamamatsu FDSS 7000, which is a kinetic fluorescence/luminescence reader typically employed for G-protein-coupled receptor (GPCR) and ion channel cell-based assay detection. In combination with the use of assay-ready plates, the integration of an FDSS 7000 with an Agilent Biocel 900 that automated the reagent addition created an efficient linear plate flow that permitted the extreme HTS of 320,000 wells per day. The absence of separate compound plates also doubled the effective storage capacity for assay plates for this fairly small footprint system ($\sim 3 \text{ m}^2$). The baseline fluorescence of the assay plates that contained 8 μl of test compound and LDHA pre-bound to NADH in assay buffer was measured for 5 s after the plates were loaded into the FDSS 7000. Compounds that altered the NADH fluorescence baseline were flagged as potential fluorescent artifacts. Using a 1536-well dispensing tip head, 2 μl of concentrated pyruvate (5 \times) was added to initiate the enzymatic reaction and the change in NADH fluorescence was recorded for 3 min. The activity of the enzyme was analyzed in a Genedata Kinetic Analyzer and defined by the slope of NADH fluorescence decay between 60 and 120 s, which was the linear range of the observed enzyme reaction (Fig. 3A).

Apparent K_m determination in both mass spectrometric and NADH fluorescence assays

Using both the NADH fluorescence kinetic assay and mass spectrometric detection, the apparent substrate K_m values were

determined against LDHA (Fig. 3B and C). The apparent K_m values of NADH were 6 μM in the NADH fluorescence assay (in the presence of 200 μM pyruvate) and 14 μM in the mass spectrometric assay (in the presence of 500 μM pyruvate). The apparent K_m values for pyruvate were 56 μM in the NADH fluorescence assay (with 50 μM NADH) and 120 μM in the mass spectrometric assay (with 500 μM NADH). Overall, the apparent K_m values obtained from the two assays are within the range of reported values for LDHA (pyruvate $K_m = 55\text{--}350 \mu\text{M}$ and NADH $K_m = 5\text{--}35 \mu\text{M}$) [21–25].

Primary screen using NADH kinetic fluorescence assay

It is known that LDHA binds to its cosubstrates in a sequential manner, with NADH binding first followed by pyruvate [13,14]. The NADH concentration in cancer cells is generally elevated and has been reported to be from 168 to 870 μM [26,27], which is significantly higher than the reported K_m value [21–25]. These data suggest that LDHA is likely bound to NADH in cancer cells. Therefore, a competitive inhibitor with NADH, such as those reported by Ward and coworkers, might generally yield poor cellular activity [28] (WO/2012/061557). Similar to pyruvate where binding to the enzyme is dependent on the presence of NADH, oxamate (a pyruvate-mimetic inhibitor) exhibited higher inhibitory potency with increasing concentrations of NADH (Fig. 3D), suggesting an uncompetitive inhibitory mechanism with the LDHA–NADH complex. These collective data led us to design our kinetic fluorescence HTS assay strategy to maximize the opportunity of finding either uncompetitive or noncompetitive inhibitors with NADH by screening our compounds in the presence of 50 μM NADH (~ 10 -fold higher than its experimental K_m). Equimolar pyruvate to NADH, which was equivalent to the pyruvate K_m value, was used.

Using the NADH kinetic fluorescence assay, a screen was successfully conducted against more than 1 million HTS compounds. The plate view of the 1536-well fluorescence kinetic traces is shown in Fig. 4A with a magnified view of representative controls and inhibitory reactions. The average Z' of the 1536-well fluorescence kinetic assay screen was 0.7 (Fig. 4B). The primary hit rate

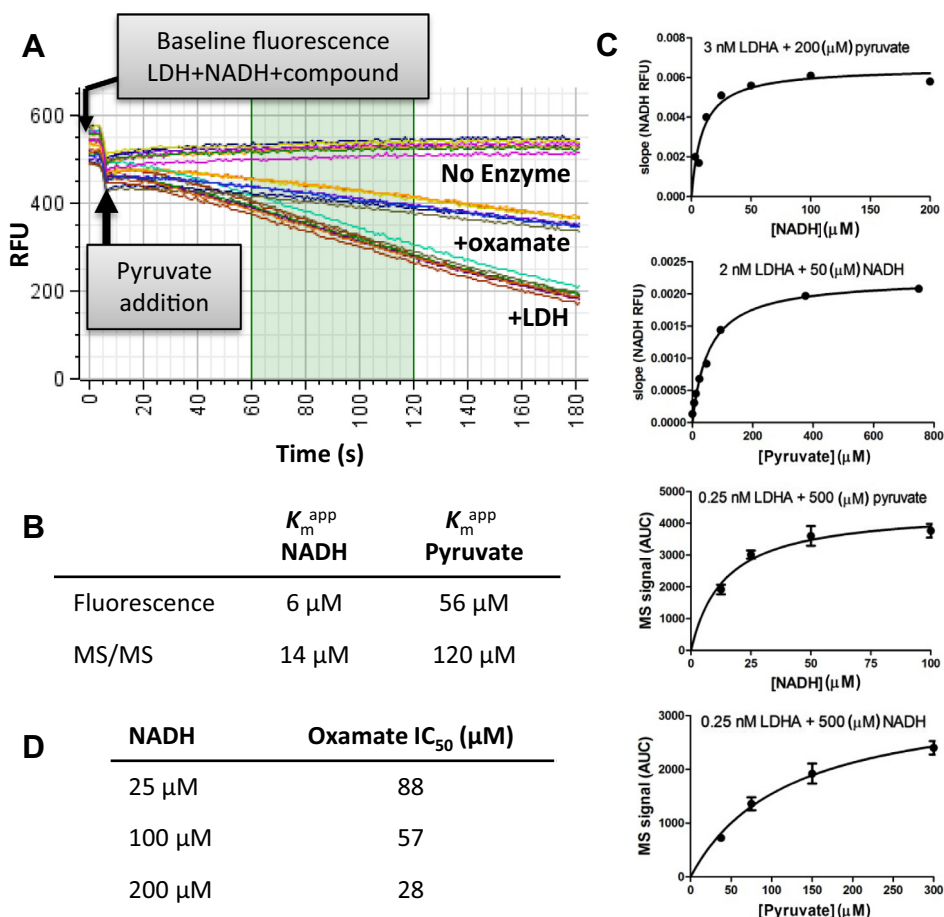


Fig. 3. (A) NADH fluorescence kinetic assay. The sequence of kinetic reaction measurement and reagent addition is shown with the kinetic traces of no-enzyme, plus LDHA, and plus LDHA and oxamate controls. The slope of the reaction was measured between 60 and 120 s highlighted in green using a Genedata Kinetic Analyzer. (B,C) Apparent K_m determination of pyruvate and NADH in the mass spectrometric and NADH fluorescence assays. MS/MS, tandem mass spectrometry. (D) IC_{50} determination of oxamate in reactions titrated with NADH.

corresponding to the number of compounds that yielded at least 50% inhibition in the rate of LDHA-mediated NADH fluorescence decrease was 0.3%. This preliminary hit rate was high considering that this enzyme class is not known to be a highly druggable target by HTS against a small molecule library [28]. When the baseline fluorescence of NADH in the presence of compounds was compared with the apparent decrease of the NADH depletion, as expected, a significant number of primary hits fluoresced at wavelengths that overlapped with NADH fluorescence (Fig. 4C). In fact, a series of compounds were found to have a positive correlation of fluorescence intensity with apparent percentage inhibition. The overall high fluorescence intensity of those compounds put the NADH fluorescence out of the linear detection range of the FDSS 7000, which resulted in a smaller than anticipated change in NADH fluorescence intensity during the enzymatic reaction. The primary hits that had a combined baseline fluorescence of less than 500 RFU were prioritized for IC_{50} confirmation, and the hit rate after applying this fluorescence cutoff decreased 5-fold to 0.06%, a value expected for this enzyme target class when screened against the Genentech HTS library.

With a primary screen conducted using a kinetic NADH fluorescence assay, we believe that we have effectively eliminated the majority of fluorescence artifacts that could create false positives in HTS. By directly measuring NADH to NAD^+ conversion instead of using coupling enzyme detection, the HTS assay we have chosen also had prevented another major source of false positives—those compounds that may preferentially inhibit the coupling enzyme

reaction or detection. Even though this primary screen approach can effectively lower the number of compound hits that interfere with assay format-specific detection, it does not prevent other types of undesirable inhibitors such as covalent modifiers and redox reactive compounds. To help prioritize validated hits that will likely yield evaluable SAR (Structural-Activity Relationship), a post-HTS triage cascade was put into place (Fig. 5). On completion of IC_{50} confirmation in the NADH fluorescence kinetic assay, the confirmed hits were further tested in the mass spectrometric assay that detects the other half of the reaction (conversion of pyruvate to lactate) and a few selected hits also underwent mechanistic characterization to probe their reversibility and substrate competition. In the next sections, we describe the characterizations of various inhibitors identified from the screen.

Irreversible inhibitory hits

Among the primary hits that were confirmed in the dose–response study using the NADH kinetic fluorescence assay, a significant number of compounds were found to contain a carboxylic acid moiety and, therefore, were predicted to bind to the pyruvate substrate site. Among the acid-containing hits, compound A, which shared a similar compact structure as the pyruvate-mimic inhibitor oxamate, yielded similar inhibitory potency as oxamate in the presence of 50 μ M pyruvate and 50 μ M NADH using the NADH fluorescence kinetic assay (Fig. 6A). Surprisingly, however, at an elevated level of pyruvate (500 μ M), the IC_{50} value of compound

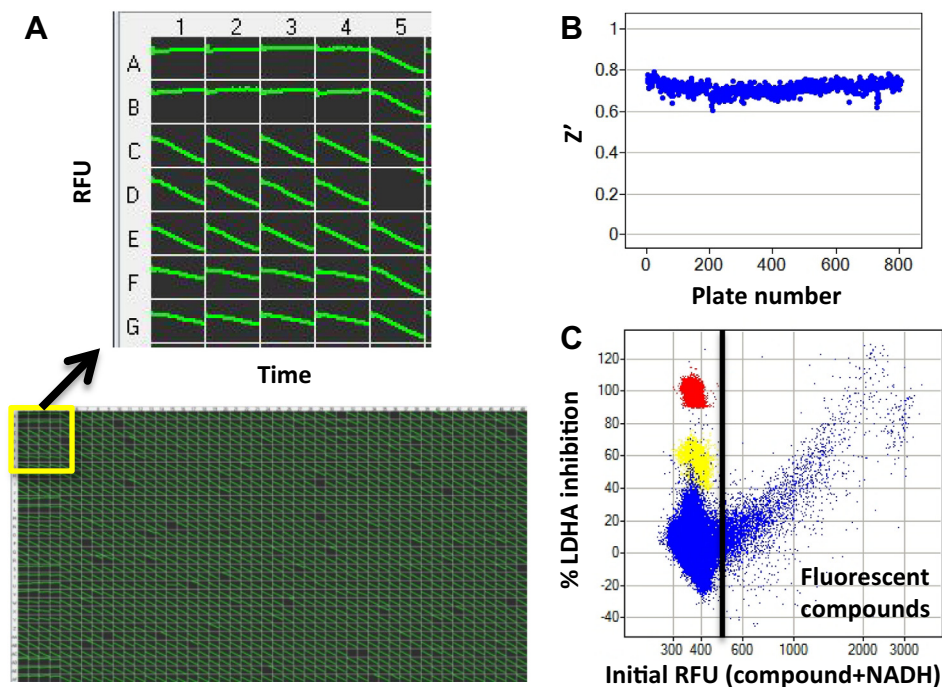


Fig. 4. LDHA primary screen. (A) Representative kinetic traces of LDHA reactions carried out in a 1536-well microplate. Examples of no-enzyme controls (rows A and B and columns 1–4), positive enzyme controls (rows C–E and columns 1–4), control compound oxamate inhibition (rows F and G and columns 1–4), and library compounds (rows A–G and column 5) are shown in the magnified view. (B) Z' values of all plates in the screen. (C) Correlation of LDHA percentage inhibition and the baseline fluorescence intensity of NADH with compound measured at initial 5 s: no-enzyme control (red), oxamate control inhibition (yellow), enzyme positive control (green), and library compound (blue). A significant number of fluorescent compounds were found to have positive correlation with the apparent LDHA inhibition.

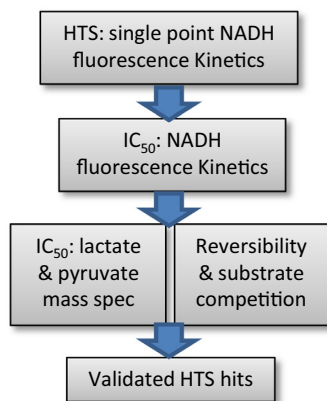


Fig. 5. HTS primary screen and hit triage cascade for LDHA.

A was the same as that observed at 50 μM pyruvate (IC_{50} values = 13 and 14 μM , respectively), whereas the IC_{50} value of oxamate was shifted weaker on an increase in pyruvate concentration (IC_{50} values = 18 μM at 50 μM pyruvate and 153 μM at 500 μM pyruvate), as would be expected for a pyruvate-competitive inhibitor. This noncompetitive mechanism of compound A with respect to pyruvate suggested that compound A may bind to a different site in spite of the structural similarity. An alternative hypothesis would be that compound A might be an irreversible inhibitor that can covalently modify the enzyme. This is a distinct possibility because it has been previously reported that the transient dissociation of the LDH tetramer can render the protein susceptible to irreversible inactivation by iodoacetamide [29]. To investigate the hypothesis, compound A was tested side by side with oxamate to assess the reversibility of its inhibitory activity. Both 100 nM

LDHA and 62.5 μM NADH were incubated with 100 μM compound A or 200 μM oxamate, concentrations approximately 10-fold higher than their respective IC_{50} values, and the reaction mixture showed the expected full inhibition measured by the NADH fluorescence assay (Fig. 6B and C). After 30 min of incubation, the enzyme–inhibitor complexes were diluted 50-fold into a buffer containing only 62.5 μM NADH to reach the compound concentrations 5-fold below their IC_{50} values, and the inhibitory potencies were immediately measured on the addition of pyruvate substrate. The enzyme that was incubated with oxamate showed full recovery of catalytic activity (to the level of the DMSO control) (Fig. 6D), whereas the reaction that contained the compound A dilution yielded full inhibition, on par with the level seen with predilution (Fig. 6E). Similar enzyme activities were observed at later time points of 1 and 2 h postdilution (data not shown), suggesting that compound A is indeed an irreversible inhibitor. This result is consistent with the observed noncompetitive mechanism of compound A with the pyruvate substrate. It is hypothesized that the thiophene might not be stable because discoloration was observed in a 10-mM DMSO stock solution over a few weeks and might present a reactive moiety to LDHA. Together, the data represent a good case study illustrating the importance of mechanistic follow-up in confirming hits obtained from an HTS campaign even if the hits share similar structures with known inhibitors and are presumed to interact with the protein in a similar binding mode.

HTS follow-up triage using the mass spectrometry assay to validate LDHA inhibitors

As described in previous sections, a primary screen was conducted using an NADH fluorescence kinetic assay against the Genentech HTS library. Primary hits were selected for IC_{50} confirmation based on percentage inhibition, and those hits that showed minimal fluorescence interference with NADH fluorescence were

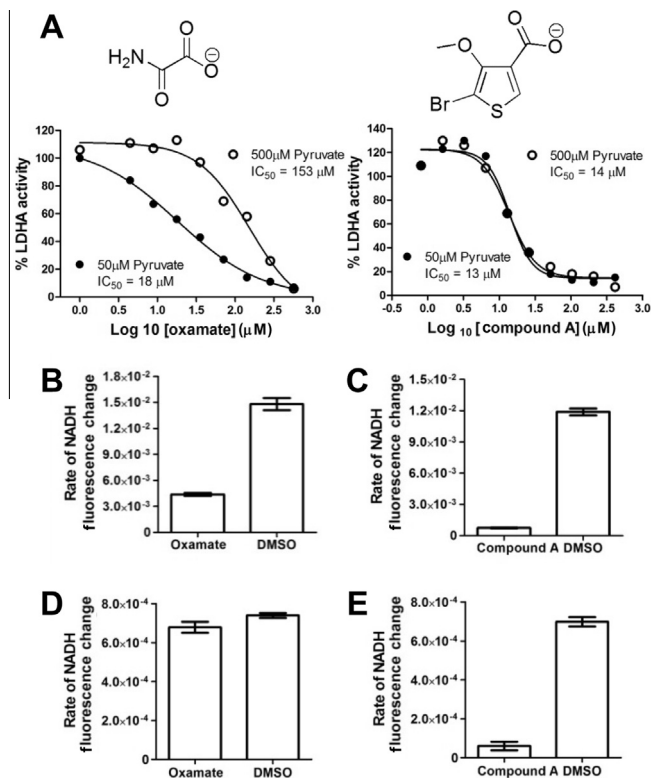


Fig. 6. Characterization of LDHA inhibition by oxamate and compound A in the NADH fluorescence assay. (A) Oxamate and compound A were tested at two different concentrations of pyruvate. (B–E) Inhibitory reversibility study of oxamate and compound A. Both 200 μM oxamate (B) and 100 μM compound A (C) (concentration 10-fold higher than their respective IC₅₀ values) were incubated with 100 nM LDHA, and both showed 70% to nearly 100% inhibition of the LDHA activity relative to the DMSO control. After rapid dilution to reach a concentration 5-fold below their respective IC₅₀ values, oxamate (D) showed immediate recovery of LDHA activity, whereas compound A (E) showed less than 10% residual LDHA activity.

prioritized. Numerous selected hits were confirmed to have dose-dependent inhibition in the fluorescence kinetic assay, with some

compounds reaching sub-micromolar potency. Among the confirmed hits, there were a few compounds showing a moderate degree of fluorescence interference at concentrations significantly higher than the reported IC₅₀ values; these compounds were included in the set prioritized for further follow-up assays. When this set of hits was tested in the mass spectrometric assay, a solid correlation of IC₅₀ values was observed for compounds that demonstrated inhibitory potency in both assays (Fig. 7A). Among those compounds that were flagged to have fluorescence interference at a high compound concentration (Fig. 7A, red circles), only 18% of them were confirmed in the mass spectrometric assay, suggesting that many were indeed false positive compounds due to fluorescence interference. This number was in contrast to the 72% confirmation rate among compounds that did not show fluorescence interference at all concentrations tested (Fig. 7A, blue circles). In addition to identifying fluorescent false positive hits, the mass spectrometric data also revealed a new class of artificial inhibitors of the LDHA reaction. For an on-target enzyme inhibition, the titration of the compound is expected to yield a decrease in the enzyme-mediated lactate production as well as a concomitant accumulation of the pyruvate substrate (Fig. 7B). However, a set of structurally related compounds decreased generation of lactate production and at the same time resulted in a depletion of detectable pyruvate substrate using the specific MRM method when they were incubated in the enzyme reaction (Fig. 7C). Even though the mechanism of the substrate depletion by this class of compounds is unknown, the decrease in the lactate generation was likely due to the decrease in the substrate available for enzymatic catalysis.

After confirming IC₅₀ values using the primary mass spectrometric assay, a limited set of validated inhibitors with good potency and physical-chemical properties was selected for further characterization to elucidate the mode of inhibition using the mass spectrometric assay. The compounds were tested at three different NADH and pyruvate concentrations to assess their potency in the range of NADH concentration approximate to the cellular level: (i) 75 and 75 μM, (ii) 300 and 75 μM, and (iii) 75 and 500 μM, respectively. A few compounds from this set showed a similar inhibitory profile, and an example is depicted in Fig. 7D for compound D. In the presence of an increased amount of pyruvate,

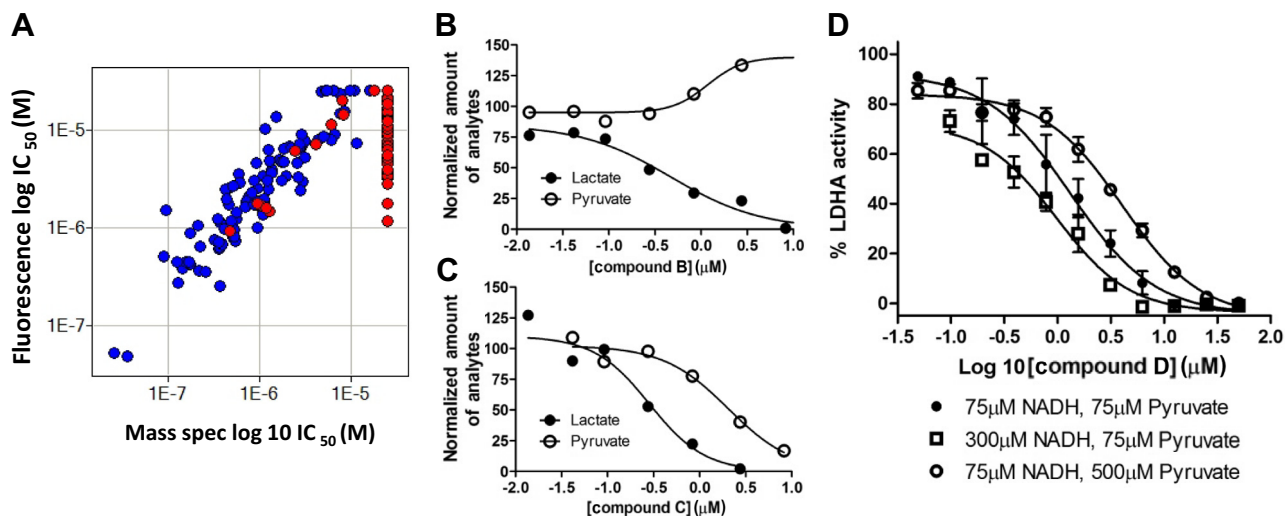


Fig. 7. (A) Better IC₅₀ correlation of LDHA inhibitors between the NADH fluorescence kinetic assay and mass spectrometric assay was observed for compounds that had no fluorescence interference (blue) relative to compounds that showed modest fluorescence interference at high concentration (red). (B) A representation of an LDHA inhibitor (compound B) that showed a concentration-dependent decrease in lactate level with a concomitant increase in pyruvate substrate. (C) An example of a substrate-depleting compound C that inhibited LDHA by decreasing the available pyruvate substrate concentration. (D) IC₅₀ values of compound D at different concentrations of pyruvate and NADH showed this compound to be competitive with pyruvate but not with NADH.

the potency of the compound was shifted weaker (IC_{50} values = 1.3 ± 0.2 and $4.5 \pm 0.4 \mu\text{M}$ for 75 and 500 μM pyruvate, respectively), suggesting that compound D might be occupying the pyruvate binding site. At an elevated concentration of NADH, compound D did not lose potency and in fact might have exhibited a very modest increase in inhibition ($IC_{50} = 0.9 \pm 0.2 \mu\text{M}$). These data confirmed an inhibitory mechanism that is competitive only with pyruvate and not NADH. Furthermore, the result does not rule out potential uncompetitive inhibition with respect to the LDHA–NADH complex. Because of the concomitant increase in the affinity of pyruvate on the increase of NADH concentration, the apparent potency gain of an inhibitor that is uncompetitive with NADH but competitive with pyruvate can be affected. Due to the limit of detection in both assays, it was not feasible to further validate the potential NADH-uncompetitive mechanism of this set of compounds, including compound D, by demonstrating a significant loss of potency using NADH concentration significantly lower than its apparent K_m ; however, this pyruvate site binding mode was later confirmed by cocrystal structures of a few representative inhibitors preferentially bound to the enzyme complex with NADH [30,31].

Conclusions

A strategically designed kinetic high-throughput screen measuring NADH fluorescence coupled with a novel mass spectrometric assay that readily provides quantitative analysis of lactate and pyruvate was able to efficiently capture both sides of the LDHA reaction, eliminate fluorescent artifacts and pyruvate-depleting compounds, and (most important) identify inhibitors that are either noncompetitive or uncompetitive with the LDHA–NADH complex. Whether a small molecule selective inhibitor that does not compete with NADH binding will provide better efficacy in cells compared with an NADH-competitive inhibitor will be the focus of future studies. If demonstrated to be more effective in cells than previously reported NADH site LDHA inhibitors, the elaboration of these HTS hits will also provide valuable tool compounds to aid the validation of LDHA's role in glycolytically addicted cancer cells and tumor metabolism.

Acknowledgments

We thank the entire baculovirus expression group and protein chemistry department at Genentech for cloning, expressing, and purifying many of the enzymes used in the study, particularly Krista Bowman, Yvonne Franke, Mike Elliott, and Jiansheng Wu. We also thank Mark Ultsch for providing initial protein samples for preliminary enzymatic characterization.

References

- [1] W.G. Kaelin Jr., C.B. Thompson, Cancer: clues from cell metabolism, *Nature* 465 (2010) 562–564.
- [2] D.A. Tennant, R.V. Duran, E. Gottlieb, Targeting metabolic transformation for cancer therapy, *Nat. Rev. Cancer* 10 (2010) 267–277.
- [3] P.S. Ward, C.B. Thompson, Metabolic reprogramming: a cancer hallmark even Warburg did not anticipate, *Cancer Cell* 21 (2012) 297–308.
- [4] N. Zaidi, J.V. Swinnen, K. Smans, ATP–citrate lyase: a key player in cancer metabolism, *Cancer Res.* 72 (2012) 3709–3714.
- [5] C.R. Santos, A. Schulze, Lipid metabolism in cancer, *FEBS J.* 279 (2012) 2610–2623.
- [6] W.H. Koppenol, P.L. Bounds, C.V. Dang, Otto Warburg's contributions to current concepts of cancer metabolism, *Nat. Rev. Cancer* 11 (2011) 325–337.
- [7] O. Warburg, On the origin of cancer cells, *Science* 123 (1956) 309–314.
- [8] J. Vamecq, J.M. Colet, J.J. Vanden Eynde, G. Briand, N. Porchet, S. Rocchi, PPARs: interference with Warburg effect and clinical anticancer trials, *PPAR Res.* 2012 (2012) 304760.
- [9] J.W. Kim, C.V. Dang, Cancer's molecular sweet tooth and the Warburg effect, *Cancer Res.* 66 (2006) 8927–8930.
- [10] A. Le, C.R. Cooper, A.M. Gouw, R. Dinavahi, A. Maitra, L.M. Deck, R.E. Royer, D.L. Vander Jagt, G.L. Semenza, C.V. Dang, Inhibition of lactate dehydrogenase A induces oxidative stress and inhibits tumor progression, *Proc. Natl. Acad. Sci. USA* 107 (2010) 2037–2042.
- [11] L. Zhuang, R.A. Scolyer, R. Murali, S.W. McCarthy, X.D. Zhang, J.F. Thompson, P. Hersey, Lactate dehydrogenase 5 expression in melanoma increases with disease progression and is associated with expression of Bcl-XL and Mcl-1, but not Bcl-2 proteins, *Mod. Pathol.* 23 (2010) 45–53.
- [12] M. Zhou, Y. Zhao, Y. Ding, H. Liu, Z. Liu, O. Fodstad, A.I. Riker, S. Kamarajugadda, J. Lu, L.B. Owen, S.P. Ledoux, M. Tan, Warburg effect in chemosensitivity: targeting lactate dehydrogenase-A re-sensitizes taxol-resistant cancer cells to taxol, *Mol. Cancer* 9 (2010) 33.
- [13] J. Sudi, Macroscopic rate constants involved in the formation and interconversion of the two central enzyme–substrate complexes of the lactate dehydrogenase turnover, *Biochem. J.* 139 (1974) 261–271.
- [14] J. Sudi, The lactate dehydrogenase–reduced nicotinamide–adenine dinucleotide–pyruvate complex: kinetics of pyruvate binding and quenching of coenzyme fluorescence, *Biochem. J.* 139 (1974) 251–259.
- [15] B.S. Khominskii, Histochemistry of the oxidation–reduction enzymes in the cells of neuroectodermal tumors, *Arkh. Patol.* 37 (1975) 10–17.
- [16] V.R. Fantin, J. St-Pierre, P. Leder, Attenuation of LDH-A expression uncovers a link between glycolysis, mitochondrial physiology, and tumor maintenance, *Cancer Cell* 9 (2006) 425–434.
- [17] S.R. Choi, A. Pradhan, N.L. Hammond, A.G. Chittiboyina, B.L. Tekwani, M.A. Avery, Design, synthesis, and biological evaluation of *Plasmodium falciparum* lactate dehydrogenase inhibitors, *J. Med. Chem.* 50 (2007) 3841–3850.
- [18] S.R. Choi, A.B. Beeler, A. Pradhan, E.B. Watkins, J.M. Rimoldi, B. Tekwani, M.A. Avery, Generation of oxamic acid libraries: antimalarials and inhibitors of *Plasmodium falciparum* lactate dehydrogenase, *J. Comb. Chem.* 9 (2007) 292–300.
- [19] S.G. Golshani-Hebroni, S.P. Bessman, Hexokinase binding to mitochondria: a basis for proliferative energy metabolism, *J. Bioenerg. Biomembr.* 29 (1997) 331–338.
- [20] A. Zhu, R. Romero, H.R. Petty, A sensitive fluorimetric assay for pyruvate, *Anal. Biochem.* 396 (2010) 146–151.
- [21] A. Chaikuad, V. Fairweather, R. Connors, T. Joseph-Horne, D. Turgut-Balik, R.L. Brady, Structure of lactate dehydrogenase from *Plasmodium vivax*: complexes with NADH and APADH, *Biochemistry* 44 (2005) 16221–16228.
- [22] M.S. Gomez, R.C. Piper, L.A. Hunsaker, R.E. Royer, L.M. Deck, M.T. Makler, D.L. Vander Jagt, Substrate and cofactor specificity and selective inhibition of lactate dehydrogenase from the malarial parasite *P. falciparum*, *Mol. Biochem. Parasitol.* 90 (1997) 235–246.
- [23] B. Quistorff, N. Grunnet, The isoenzyme pattern of LDH does not play a physiological role: except perhaps during fast transitions in energy metabolism, *Aging* 3 (2011) 457–460.
- [24] I. Baskakov, A. Wang, D.W. Bolen, Trimethylamine-N-oxide counteracts urea effects on rabbit muscle lactate dehydrogenase function: a test of the counteraction hypothesis, *Biophys. J.* 74 (1998) 2666–2673.
- [25] B.F. Howell, S. Margolis, R. Schaffer, Detection of inhibitors in reduced nicotinamide adenine dinucleotide by kinetic methods, *Clin. Chem.* 22 (1976) 1648–1654.
- [26] S. Villette, S. Pigaglio-Deshayes, C. Vever-Bizet, P. Validire, G. Bourg-Heckly, Ultraviolet-induced autofluorescence characterization of normal and tumoral esophageal epithelium cells with quantitation of NAD(P)H, *Photochem. Photobiol. Sci.* 5 (2006) 483–492.
- [27] Q. Yu, A.A. Heikal, Two-photon autofluorescence dynamics imaging reveals sensitivity of intracellular NADH concentration and conformation to cell physiology at the single-cell level, *J. Photochem. Photobiol., B* 95 (2009) 46–57.
- [28] R.A. Ward, C. Brassington, A.L. Breeze, A. Caputo, S. Critchlow, G. Davies, L. Goodwin, G. Hassall, R. Greenwood, G.A. Holdgate, M. Mrosek, R.A. Norman, S. Pearson, J. Tart, J.A. Tucker, M. Vogtherr, D. Whittaker, J. Wingfield, J. Winter, K. Hudson, Design and synthesis of novel lactate dehydrogenase A inhibitors by fragment-based lead generation, *J. Med. Chem.* 55 (2012) 3285–3306.
- [29] J. Sudi, M.G. Khan, Transient dissociation of lactate dehydrogenase resulting in increased reactivity towards iodoacetamide, *FEBS Lett.* 6 (1970) 253–256.
- [30] P.S. Dragovich, B.P. Fauber, L.B. Corson, C.Z. Ding, C. Eigenbrot, H. Ge, A.M. Giannetti, T. Hunsaker, S. Labadie, Y. Liu, S. Malek, B. Pan, D. Peterson, K. Pitts, H.E. Purkey, S. Sideris, M. Ultsch, E. VanderPorten, B. Wei, Q. Xu, I. Yen, Q. Yue, H. Zhang, X. Zhang, Identification of substituted 2-thio-6-oxo-1,6-dihydropyrimidines as inhibitors of human lactate dehydrogenase, *Bioorg. Med. Chem. Lett.* 23 (2013) 3186–3194.
- [31] B.P. Fauber, P.S. Dragovich, J. Chen, L.B. Corson, C.Z. Ding, C. Eigenbrot, A.M. Giannetti, T. Hunsaker, S. Labadie, Y. Liu, Y. Liu, S. Malek, D. Peterson, K. Pitts, S. Sideris, M. Ultsch, E. VanderPorten, J. Wang, B. Wei, I. Yen, Q. Yue, Identification of 2-amino-5-aryl-pyrazines as inhibitors of human lactate dehydrogenase, Manuscript in preparation.